Advances in Applied Physics, Vol. 7, 2019, no. 1, 19 – 28 HIKARI Ltd, www.m-hikari.com https://doi.org/10.12988/aap.2019.985

Photoluminescence of Ag-Loaded A, X, and Y Type

Zeolites Heat-Treated in Atmosphere

Yushi Suzuki*, Takafumi Miyanaga, Kazuma Yamauchi, Naohiro Mori and Reki Nakamura

Department of Mathematics and Physics Graduate School of Science and Technology Hirosaki University, Hirosaki, Aomori, Japan *Corresponding author

This article is distributed under the Creative Commons by-nc-nd Attribution License. Copyright © 2019 Hikari Ltd.

Abstract

We use in-situ X-ray absorption fine structure (XAFS) to examine the relation between Ag clusters or Ag ions and properties of photoluminescence (PL). The Ag clusters are generated in the cavity of Ag-type zeolite-A, X, and Y heating in atmosphere. The Ag clusters in the zeolite cavity break down when cooled to room temperature after heating in atmosphere. Results of this study suggest that collapsing Ag cluster plays an important role in the generation of strong PL bands and that Ag clusters might not be a direct species of PL. Results also show that the local sites of Ag ions differ slightly from the unheated species induced by the formation and destruction of Ag clusters.

Keywords: Ag cluster, Photoluminescence, XAFS, Zeolite

1 Introduction

Zeolites are crystalline aluminosilicates that exhibit unique properties because of the presence of large ordered cavities (cages) in their structure [10, 15, 16, 24]. They have been widely used in applications such as catalysis, ion exchange, and separation [2, 7, 18, 23, 25]. Furthermore, zeolite is an inexpensive material. A promising property of Ag⁺ exchanged zeolite is its photoluminescence (PL). In fact, Ag-zeolite is a luminescent material despite having no rare earth metal constituent. Recently, many researchers have explored the emissive behaviour of silver-exchanged zeolite [3, 4, 8, 11-13, 21, 22]. Various reports have explained that the

photoluminescence of Ag-zeolite derives from Ag clusters formed in the zeolite framework. Silver cluster formation has been confirmed from studies using inorganic substances such as silica as matrix [1, 14]. However, studies of PL of zeolite have only indirectly confirmed the presence of Ag clusters. For an earlier study, we took PL and XAFS measurements of zeolite-A to ascertain the relation between the PL band and the local structure of the Ag cluster [19, 20]. Results confirmed that Ag clusters are formed during heat treatment processing. Then the Ag clusters are broken down when cooled to room temperature (RT). In fact, XAFS measurements of the unheated XAFS spectrum and the cooled spectra are very similar. No PL band from unheated Ag-zeolite-A was observed, but the heat-treated sample exhibits strong PL bands. To date, we have measured the PL using excitation light from 405 nm LEDs and semiconductor lasers. Those results have shown the relation between "state of Ag by XAFS" and PL. Elucidating the PL mechanism of Ag type zeolites necessitates clarification of the relation between PL excited by other wavelengths and the Ag state. The present study was conducted to observe PL using excitation light at 220-700 nm and to assess results of XAFS measured under the same conditions, thereby elucidating the PL mechanisms of zeolite-A. -X. and -Y.

2 Experimental

Na-type zeolite zeolite-A (Na₁₂[(AlO₂)₁₂(SiO₂)₁₂]), X (Na₈₆[(AlO₂)₈₆(SiO₂)₁₀₆]), and Y (Na_{51.2}[(AlO₂)_{51.2}(SiO₂)_{140.8}]) powder samples were purchased from TOSOH Co. Ltd.. Fully Ag-exchanged powder samples were prepared using ion-exchange method. The Ag-type zeolites were heated at 400 - 700 °C under atmosphere to produce the Ag cluster. Then PL measurements were taken using a UV-VIS spectrometer (F-2700; Hitachi High-Technologies Corp.). All measurements were taken at RT.

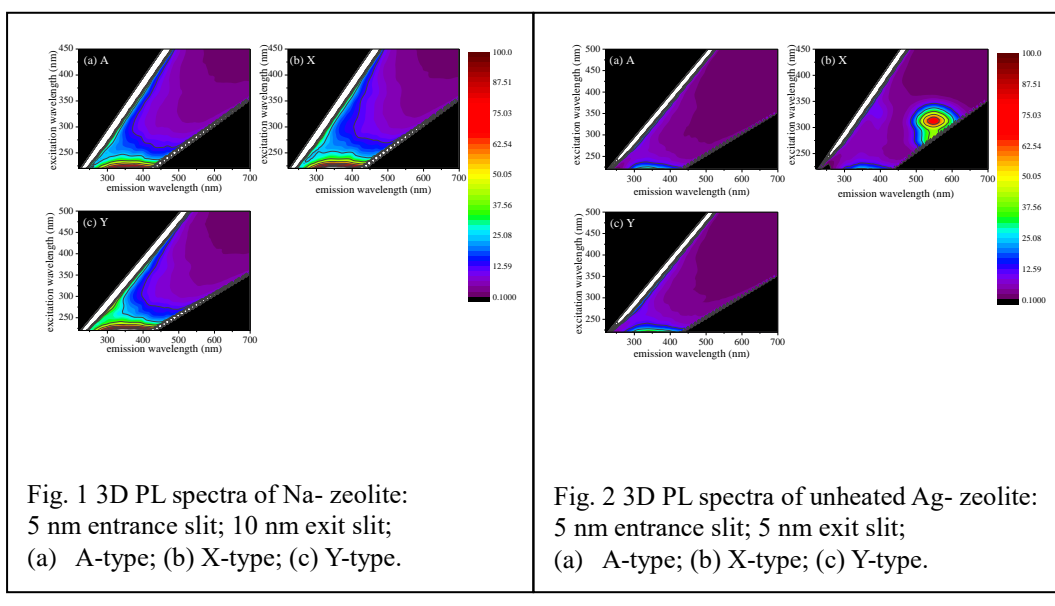
The X-ray absorption spectra of K-edge of Ag (25 keV) were measured at NW10A of the Photon Factory at KEK using transmission mode. We used XANADU code and FEFF 8.10 for XAFS analyses.

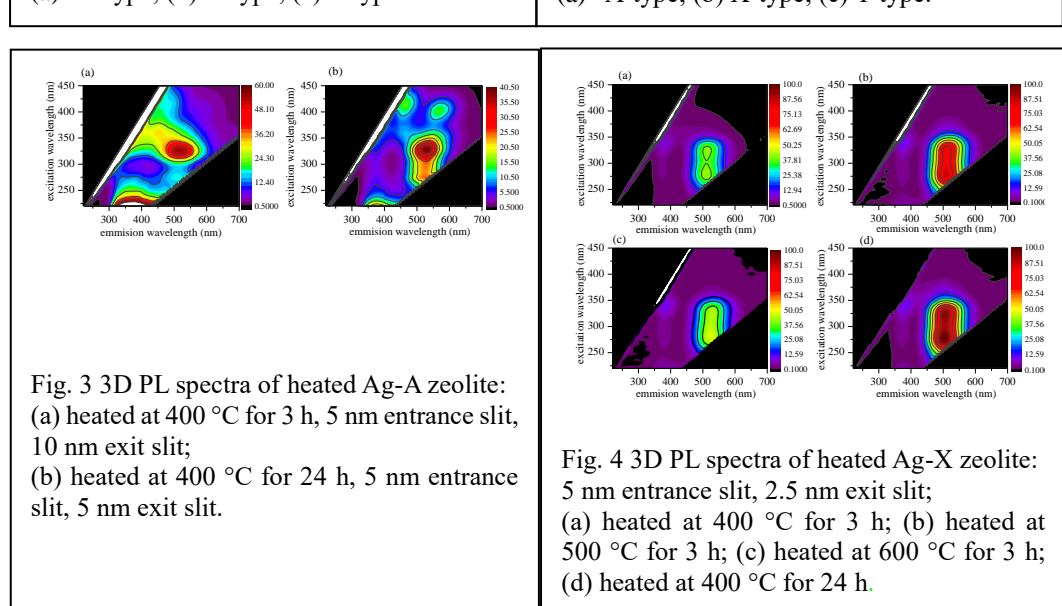
Ag-type zeolites were heated at 400 - 700 °C for 3 h or 24 h in atmosphere to produce Ag clusters [19]. Experimental details are presented in reports of several earlier studies [9, 17].

3 Results and Discussion

First, we present PL measurement results. Figure 1 presents 3D PL spectra of Nazeolite, confirming that the PL at around 350 nm at 220 nm excitation depends on the zeolite framework. This PL band is not mentioned hereinafter.

Figure 2 portrays the 3D PL spectra of unheated Ag-loaded zeolite. Weak PL of 550 nm is observed at 325 nm excitation in X-type only. It is clearer than the 350 nm





PL band derived from the zeolite framework. In A-type and Y-type, only PL derived from zeolite framework is observed.

3D PL spectra of heated Ag–A zeolite are shown in figure 3. Noticeable PL was observed irrespective of the heating time. With heating for 3 h, a main peak is observed at 520 nm (325 nm excitation wavelength); its base extends to the shorter wavelength side. Moreover, with heating for 24 h, a main peak was observed at 530 nm (330 nm excitation wavelength), and PL of the same 530 nm is observed for widely various excitation wavelengths of 270–360 nm. In addition, subpeaks were

newly observed at around 465 nm (415 nm excitation wavelength) and 565 nm (400 nm excitation wavelength). The excitation wavelength of the subpeak was revealed as around 400 nm. That observed at the excitation wavelength 405 nm was this subpeak [9, 17, 19, 20]. The main peak strength increased with heating time: the base which was visible after heating for 3 h weakened.

The 3D PL spectra of heated Ag-X zeolite are portrayed in figure 4. Clear PL was observed around 510 nm over wide excitation wavelengths 250-330 nm. For Ag-X, even if the heating temperature and heating time were changed, the PL wavelength did not change substantially. Only the PL intensity changed. With heating for 3 h, the maximum intensity was reached by heating at 500 °C. Actually, PL that was stronger than the heating for 3 h observed at 24 h heating. Furthermore, the excitation efficiency drops slightly near 300 nm excitation wavelength, indicating that excitation peaks show the same PL around 300 nm.

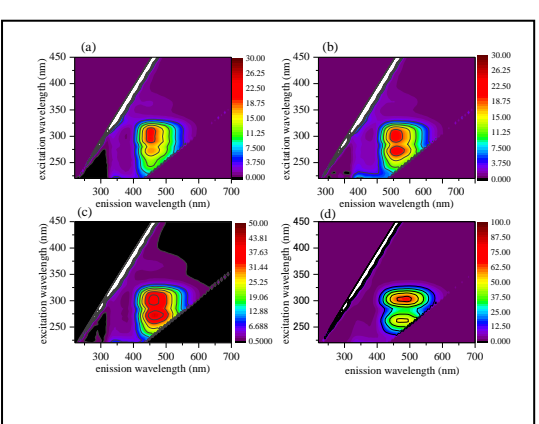


Fig. 5 3D PL spectra of heated Ag-Y zeolite: 5 nm entrance slit; 2.5 nm exit slit; (a) heated at 400 °C for 3 h; (b) heated at 500 °C for 3 h; (c) heated at 600 °C for 3 h; (d) heated at 700 °C for 3 h.

The 3D PL spectra of heated Ag-Y zeolite are shown in figure 5. The Ag-Y result resembles the result obtained for Ag-X. Clear PL is observed around 465 nm over a wide range of excitation wavelengths: 240–325 nm. For Ag-Y, the PL wavelength was independent of the heating temperature; only the PL intensity was dependent. The PL intensity reached its maximum with heating at 700 °C. Similarly to Ag-X, the excitation efficiency drops slightly in the central excitation range, at around 280 nm. For Ag-Y, two excitation peaks show the same PL. It is noteworthy that separation of these two excitation peaks was clarified by heating at 700 °C.

Next, we present XAFS results. Figure 6 shows XANES spectra of the Ag–K edge for Ag-loaded A, X, and Y type zeolites unheated at RT in atmosphere (solid line), heated at 400 or 500 °C (dashed line), and cooled to RT after heating (dotted line). XANES reflects the electronic state of the target element. The electronic state of Ag changes during heating in A, X, and Y. After cooling to RT, it is almost identical to that in the unheated case. The electronic state with development of strong PL closely resembles the state before heating.

Figure 7 shows the Ag-K EXAFS $k^2\chi(k)$ spectra for Ag-loaded A, X, and Y type zeolites unheated at RT in atmosphere (solid line), heated at 400 or 500 °C (dashed line), and cooled to RT after heating (dotted line). For A, X, and Y, the structure around 3.5 Å ⁻¹ presents a characteristic change in the spectrum during heating, which is a structure showing the Ag cluster formation [9]. The fact that the $k^2\chi(k)$ spectrum cooled to RT after heating is almost identical to those unheated indicates that Ag clusters generated during the heating process were destroyed as described



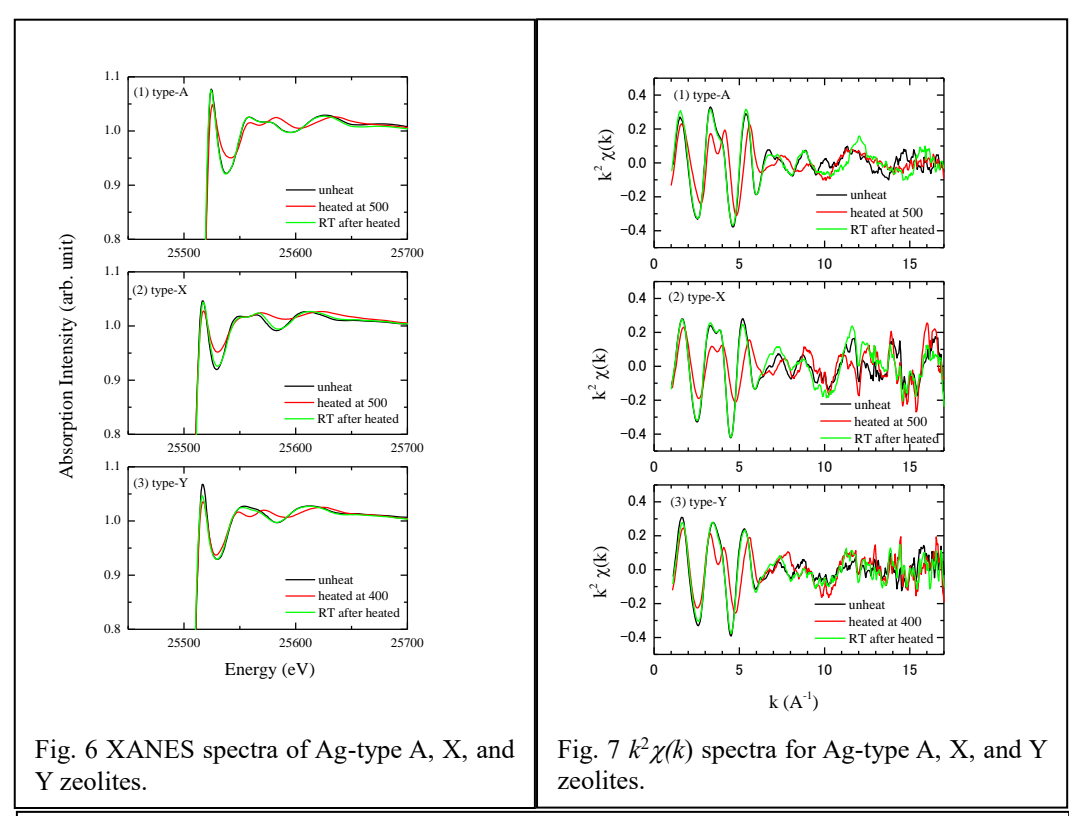


Table 1. Structural parameters: r, N, and σ for zeolite-A for the process heated under atmospheric conditions

	$r_{\mathrm{Ol}}(\mathrm{\AA})$	$N_{\rm O1}$	$r_{\rm O2}({ m \AA})$	$N_{\rm O2}$	$r_{ m Ag}(m \AA)$	N_{Ag}
Unheated sample measured at RT	2.38	3.7	2.87	0.9	2.87	1.3
Heated at 500 °C 24 h	2.28	3.3	2.70	1.7	2.81	3.1
Cooled to RT after heating in air	2.37	3.4	2.82	1.1	2.87	1.2

Table 1 presents structural parameters of r and N for O_1 , O_2 and Ag for Ag-A for the process heated at atmospheric condition. With heating, r_{O1} decreases from 2.38 Å to 2.28 Å; N_{O1} is also reduced from 3.65 to 3.25, reflecting the removal of adsorbed water molecules in the cavity. Even in the unheated species, a small portion of Ag-Ag contact exists naturally in the cavity (r_{Ag} 2.87 Å and N_{Ag} is 1.3). During the heating process, N_{Ag} increases from 1.3 to 3.1, which reflects the Ag cluster formation. The cluster size is almost identical to the Ag_4 cluster, as reported from an earlier study [6]. For this stage, Ag-A shows no strong PL yet.

The water molecules are again incorporated into the cavity during the final process of cooling to RT after heating at 500 °C. The parameters differ slightly, but are almost identical to those of the unheated case. For example, $N_{\rm OI}$ (3.4) and $N_{\rm Ag}$ (1.2) are smaller than the original unheated species. It is noteworthy that the cooled

species show strong enhancement of PL.

Table 2 presents structural parameters for Ag-X for the process of heating in an

	$r_{\mathrm{Ol}}(\mathrm{\AA})$	$N_{\rm O1}$	$r_{\rm O2}({ m \AA})$	$N_{\rm O2}$	$r_{\mathrm{Ag}}(\mathrm{\AA})$	$N_{ m Ag}$
Unheated sample measured at RT	2.38	3.8	3.06	0.7	2.98	1.7
Heated at 400 °C 24 h	2.28	3.1	2.71	1.0	2.84	2.3
Cooled to RT after heating in air	2.36	3.5	3.05	0.6	2.98	1.5
able 3. Structural parameters: r , N ,	and σ for	zeolite-	Y for the p	process h	eated at atı	mosph
*				•		•
ondition	r _{Ol} (Å)	N _{O1}	r _{O2} (Å)	N _{O2}	$r_{ m Ag}(m \AA)$	$N_{ m Ag}$
Table 3. Structural parameters: <i>r</i> , <i>N</i> , condition Unheat at Atm. pressure at RT				•		•
ondition	r _{Ol} (Å)	N _{O1}	r _{O2} (Å)	N _{O2}	$r_{ m Ag}(m \AA)$	$N_{ m Ag}$

atmospheric condition. The structural change for r_{O1} is almost identical to that of Ag-A. However, r_{O2} and r_{Ag} differ. Both are longer than that for Ag-A. Furthermore, N_{Ag} for Ag-X is smaller than that for Ag-A. These facts are dependent upon the cavity for zeolite-X being larger than that for zeolite-A. Consequently, r_{Ag} of the Ag clusters is longer than that Ag-A.

For unheated and clusters, r_{Ag} values are 2.97 Å and 2.85 Å. They are longer than those for Ag₁₂-A (2.87Å and 2.81Å). Because Ag atoms are connected strongly to oxygen atom in the framework, r_{O1} is similar to Ag-A.

Table 3 presents structural parameters for Ag-Y for the process of heating in an atmospheric condition. They are smaller than those for unheated N_{O1} (3.7) and N_{Ag} (1.3), which indicates that amount of re-adsorbed water molecule is

For zeolite-Y, r_{01} (2.36 Å) decreases to 2.31 Å by heating; N_{01} (2.7) drops to 2.3. Structural change by desorbing water molecules is slight compared to those for zeolite A and X.

The unheated N_{Ag} is remarkably small (0.2). Moreover, r_{Ag} (3.07 Å) is longer than zeolites A and X, which indicates that the Ag ions in the cavity are fewer than those of the other two that they are sparsely distributed in the zeolite Y cavity. However, the Ag cluster size produced by heating in zeolite Y is about equal to those of zeolite A and X.

The Ag ion is scattered at the same location by cooling to RT after heating. It shows almost identical structural parameters to those of the unheated species.

According to the XAFS measurement result, the Ag cluster collapsed under the condition in which strong PL was observed. The strong PL observed under the conditions in this paper might derive from the zeolite framework itself. Because zeolite is an insulator, the energy difference between the valence band and the

conduction band (the so-called band gap) is about 6 eV, which can not be the cause of PL. Zeolite has a complicated structure. Actually, theoretical calculation is difficult even for LTA (type A) and FAU (X type, Y type), which can be characterized as simple zeolites.

From theoretical calculations using clinoptilolite reported by Dong et al. [5], the following were derived.

- 1. Electrons can transition from the O-2p⁴ band to the Si-3p² conduction band.
- 2. The energy difference between O $2p^4$ and Si $3p^2$ can be approximately 2 eV.
- 3. O $2p^4$ and Si $3p^2$ bands can change about \pm 1 eV when subjected to structural damage.

Results show that $k^2\chi(k)$ spectra were changed slightly by heating. Furthermore, according to our study using Ag–A, similar infrared absorption spectra are observed before and after heating, but with some marked differences [20]. Based on these facts, we predict that the Ag⁺ ion location might have changed slightly from the unheated state and after heating because of the Ag cluster formation and collapse. The cation coordinates to the zeolite framework can be regarded as a weight hanging on the framework. Hanging the weight imposes some structural damage; changing the position of the weight (positive ion) alters the structural damage. The positions of Ag⁺ ions influence the zeolite framework differently if they change. Therefore, as described above, because of the change in the band position of O-2p⁴ and/or Si-3p²O-2p⁴, the authors infer that PL was expressed.

The hypothesis presented above can also explain the different PL energies of A, X, and Y type. The three types have a fundamental structure of a sodalite cage, which is not much different. What differs is the Si / Al ratio. For example, in the case of an A type, in which the Si / Al ratio is unity, Si and Al are arranged alternately with oxygen interposed. It can be said that the structural damage is the slightest in a structure composed of Si, Al, and O. In the X type, the Si / Al ratio is a slightly Si-rich 1.23. Therefore, the arrangement of Si–O–Al partially collapses to become Si–O–Si, whereby the strain of the structure is slightly larger than that of the A type. In the Y type, the Si / Al ratio is considerably large at 2.75. Greater structural strain than the X type exists. The structural damage increases in the order of A < X < Y. The change in the O-2p⁴ and Si-3p² bands increases according to the magnitude of the structural damage, which can explain that the PL energy increases in the order of A < X < Y.

4 Conclusion

We studied in-situ PL and XAFS of Ag-loaded A, X, and Y type zeolites to search for unknown luminescent species and to assess structural changes of Ag cluster after heat treatment in the broad excitation wavelength region. Results demonstrate that Ag clusters were formed by heat treatment and were then broken when cooled to RT. Although the main band luminescence intensity varies depending on the heating conditions, the luminescence wavelength remained almost unchanged. The

main band in each type of zeolite showed almost identical fluorescence wavelength in a wide excitation wavelength region. We speculate that a slight site change of Ag^+ ion in the zeolite cavity induced by the Ag cluster formation / collapse is a key point of the PL mechanism.

Acknowledgements. Synchrotron radiation experiments were conducted at the Photon Factory in KEK under Proposals 2011G586, 2014G054, and 2016G056. This work was supported by JPSJ KAKENHI Grant Number JP17K05026.

References

- [1] E. Borsella, E. Cattaruzza, G. De. Marchi, F. Gonella, G. Mattei, P. Mazzoldi, A. Quaranta, G. Battaglin and R. Polloni, Synthesis of silver clusters in silicabased glasses for optoelectronics applications, *Journal of Non-Crystalline Solids*, **245** (1999), 122-128. https://doi.org/10.1016/S0022-3093(98)00878-3
- [2] A. Corma, C. Corell, J. Perez-Pairente, Synthesis and characterization of the MCM-22 zeolite, Zeolites, 15 (1995), 2-8. https://doi.org/10.1016/0144-2449(94)00013-I
- [3] G.D. Cremer, E.C. Gonzalez, M.B.J. Roeffaers, B. Moens, J. Ollevier, M.V. der Auweraer, R. Schoonheydt, P.A. Jacobs, F.C. De Schryver, J. Hofkens, D.E.De Vos, B.F. Sels, T. Vosch, Characterization of Fluorescence in Heat-Treated Silver-Exchanged Zeolites, *J. Am. Chem. Soc.*, **131** (8) (2009), 3049-3056. https://doi.org/10.1021/ja810071s
- [4] E. C-Gonzalez, W. Baelelant, D. Grandjean, M.B.J. Roeffaer, E. Fron, M.S. Aghakhani, N. Bovet, M.V.der Auweraer, P. Lievens, T. Vosch, B. Sels, J. Hofkens, Thermally activated LTA(Li)–Ag zeolites with water-responsive photoluminescence properties, *J. Mater. Chem.*, C, **3** (2015), 11857-11867. https://doi.org/10.1039/c5tc02723c
- [5] F. Dong, L. Bian, M. Song, W. Li, T. Duan, Computational investigation on the fn → fn-1d effect on the electronic transitions of clinoptilolite, *Appl. Clay. Sci.*, 119 (2016), 74-81. https://doi.org/10.1016/j.clay.2015.08.042
- [6] O. Fenwick, E. Coutiño-Gonzalez, D. Grandjean, W. Baekelant, F. Richard, S. Bonacchi, D. De Vos, P. Lievens, M. Roeaers, J. Hofkens and P. Samori, Tuning the energetics and tailoring the optical properties of silver clusters confined in zeolites, *Nature Materials*, 15 (2016), 1017-1022. https://doi.org/10.1038/nmat4652

- [7] R.S. Gomez, X. Li, R.L. Yson, H.H. Patterson, Zeolite-supported silver and silver—iron nanoclusters and their activities as photodecomposition catalysts, *Res. Chem. Intermed.*, **37** (2011), 729-745. https://doi.org/10.1007/s11164-011-0313-z
- [8] S. C. R. Gui, H. Lin, W. Bao and W. Wang, Effect of Annealing Temperature on Broad Luminescence of Silver-Exchanged Zeolites Y and A, *J. Appl. Spectrosc.*, **85** (2018), 232-238. https://doi.org/10.1007/s10812-018-0637-1
- [9] H. Hoshino, Y. Sannohe, Y. Suzuki, T. Azuhata, T. Miyanaga, K. Yaginuma, M. Itoh, T. Shigeno, Y. Osawa, Y. Kimura, Photoluminescence of the Dehydrated Ag-type Zeolite A Packed under Air, *J. Phys. Soc. Jpn.*, 77 (2008), 064712. https://doi.org/10.1143/JPSJ.77.064712
- [10] Y. Kim, K. Seff, The octahedral hexasilver molecule. Seven crystal structures of variously vacuum-dehydrated fully silver(1+)-exchanged zeolite A, *J. Am. Chem. Soc.*, **100** (1978), 6989-6997. https://doi.org/10.1021/ja00490a035
- [11] S.H. Lee, Y. Kim, K. Seff, Weak Ag+—Ag+ bonding in zeolite X. Crystal structures of Ag92Si100Al92O384 hydrated and fully dehydrated in flowing oxygen, *Microporous Mesoporous Mater.*, **41** (2000), 49-59. https://doi.org/10.1016/s1387-1811(00)00270-5
- [12] H. Lin, K. Imakita, M. Fujii, V. Yu. Prokof'ev, N. E. Gordina, B. Said and A. Galarneau, Visible emission from Ag+ exchanged SOD zeolites, *Nanoscale*, **7** (2015), 15665-15671. https://doi.org/10.1039/C5NR04246A
- [13] H. Lin, K. Imakita, M. and Fujii, Reversible emission evolution from Ag activated zeolite Na-A upon dehydration/hydration, *Applied Physics Letters*, **105** (2014), 211903. https://doi.org/10.1063/1.4902530
- [14] Y.K. Mishra, S. Mohapatra, D. Kabiraj, B. Mohanta, N.P. Lalla, J.C. Pivinc and D.K. Avasthi, Synthesis and Characterization of Ag Nanoparticles in Silica Matrix by Atom Beam Sputtering, *Scripta Materialia*, **56** (2007), 629-632. https://doi.org/10.1016/j.scriptamat.2006.12.008
- [15] T. Miyanaga, H. Hoshino, H. Endo, Local structure of silver clusters in the channels of zeolite 4A, *J. Synchrotron Radiat.*, **8** (2001), 557-559. https://doi.org/10.1107/s0909049500012668
- [16] T. Miyanaga, H. Hoshino, H. Endo, H. Sakane, XAFS study of silver clusters in zeolites, J. Synchrotron Radiat., 6 (1999), 442-444. https://doi.org/10.1107/s0909049599000631

[17] T. Miyanaga, Y. Suzuki, N. Matsumoto, S. Narita, T. Ainai, H. Hoshino, Formation of Ag clusters in zeolite X studied by in situ EXAFS and infrared spectroscopy, *Microporous Mesoporous Mater.*, **168** (2013), 213. https://doi.org/10.1016/j.micromeso.2012.09.013

- [18] R.M. Mohamed, L.A. Mkhalid, M. Abdel Salam, M.A. Barakat, Zeolite Y from rice husk ash encapsulated with Ag-TiO2: characterization and applications for photocatalytic degradation catalysts, *Desalin. Water Treat.*, **51** (2013), 7562-7569. https://doi.org/10.1080/19443994.2013.775671
- [19] A. Nakamura, M. Narita, S. Narita, Y. Suzuki, T. Miyanaga, In-situ XAFS study of Ag clusters in Ag-type zeolite-A, *J. Phys.*, **502** (2014), 012033. https://doi.org/10.1088/1742-6596/502/1/012033
- [20] S. Narita, T. Miyanaga, and Y. Suzuki, IR and XAFS Studies of Photoluminescent Ag-type Zeolite-A, *Advances in Applied Physics*, **4** (2016), no. 1, 13-22. https://doi.org/10.12988/aap.2016.642
- [21] R. Seifert, R. Rytz, G. Calzaferri, Colors of Ag+-Exchanged Zeolite A, *J. Phys. Chem.*, **104** (2000), 7473-7483. https://doi.org/10.1021/jp000905z
- [22] R. Seifert, A. Kunzmann and G. Calzaferri, The Yellow Color of Silver-Containing Zeolite A, *Angew. Chem. Int. Ed.*, 37 (1998), 1521. https://doi.org/10.1002/(SICI)1521-3773(19980619)37:11<1521::AID-ANIE1521>3.0.CO;2-V
- [23] H.S. Sherry, S.M. Auerbach, K.A. Carrado, P.K. Dutta, *Handb. Zeolite Sci. Technol.*, (2003), 1007.
- [24] T. Sun, K. Seff, Silver Clusters and Chemistry in Zeolites, *Chem. Rev.*, **94** (1994), 857-870. https://doi.org/10.1021/cr00028a001
- [25] S. G. Zhang, M. Ariyuki, H. Mishima, S. Higashimoto, H. Yamashita and M. Anpo, Photoluminescence property and photocatalytic reactivity of V-HMS mesoporous zeolites Effect of pore size of zeolites on photocatalytic reactivity, *Microporous Mesoporous Mater.*, 21 (1998), 621-927. https://doi.org/10.1016/S1387-1811(98)00027-4

Received: August 23, 2019; Published: September 8, 2019